Letters

Reconfigurable Intermediate Resonant Circuit Based WPT System With Load-Independent Constant Output Current and Voltage for Charging Battery

Yong Li, Jiefeng Hu, *Senior Member, IEEE*, Ming Liu, Yang Chen, Ka Wing Chan, Zhengyou He, and Ruikun Mai

***Abstract*—In this letter, a compact battery charger based on wireless power transfer (WPT) technology without any communication requirement is proposed. Here, a new intermediate coil is developed to achieve load-independent constant current (CC) and constant voltage (CV) outputs. The intermediate coil is split into two coils and is overlapped with the receiver coil to form a compact structure. Two switches on the receiver side are used to reconfigure the intermediate resonant circuit in order to select different charging modes, i.e., CC mode or CV mode. The communication between the transmitter side and the receiver side as well as complex control strategies is not needed in the proposed structure. Besides, the proposed system can achieve zero phase angle operation, fixed operating frequency, and zero-voltage switching, which not only can lower the power rating of power devices but also improve the efficiency. A laboratory prototype with a 3.6 A charging current and a 48 V charging voltage is built to verify the feasibility of the proposed method.**

***Index Terms*—Battery, constant current (CC), constant voltage (CV), wireless power transfer (WPT).**

I. Introduction

WIRELESS power transfer (WPT) technology has been widely applied to various applications, e.g., biomedical implants [1], mining applications [2], underwater applications [3], and electric vehicles (EVs) [4] due to its crucial merits, e.g., convenient, safety, etc. In these applications, batteries are usually used to store the energy. To ensure the safety of the battery and the effectiveness of the charging system, it is desirable that a constant current (CC) charging stage is followed by a constant voltage (CV) charging stage [5]. Besides, the

Manuscript received May 13, 2018; revised June 23, 2018; accepted July 18, 2018. Date of publication July 22, 2018; date of current version February 5, 2019. This work was supported in part by the Hong Kong Polytechnic University under Grant 1-ZE7J, in part by the Hong Kong Innovation and Technology Commission under Grant ITS/281/17, and in part by the National Natural Science Foundation of China under Grant 51677155. *(Corresponding authors: Jiefeng Hu; Ruikun Mai.)*

Y. Li, J. Hu, M. Liu, and K. W. Chan are with the Department of Electrical Engineering, The Hong Kong Polytechnic University, Hong Kong (e-mail:

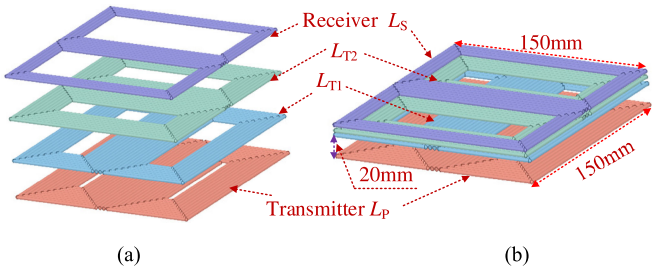

Fig. 1. Three-dimensional view of the proposed coil structure.

with the receiver coil to form a very compact structure. The intermediate coil is split into two coils. Two low-cost switches and two resonant capacitors are used in two split coils to form a reconfigurable intermediate resonant circuit. The CC and CV charging modes can be realized by reconfiguring the intermediate resonant circuit with the help of the two switches. The communication between the receiver side and the transmitter side as well as complex control methods is not needed for the proposed method. Moreover, this proposed WPT system can achieve ZPA operation, fixed operating frequency, and zero-voltage switching (ZVS) simultaneously. As a result, the power rating of the power devices will be reduced, and the efficiency will be improved.

This proposed approach is superior to the traditional methods. Compared to the approach presented in [9], this topology is more compact due to the fact that one inductor and one capacitor are saved. Compared to [10], one switch and the wireless communication are avoided. It should emphasize that the proposed structure is aimed for applications where all the parameters of the WPT system, e.g., mutual inductances and self-inductances, can be easily fixed [10], [13]. Therefore, light-weight electric mobiles, such as electric bicycles (EBs) could be a huge potential market for the proposed structure as the on-board receiver coil can be easily aligned with the stationary transmitter.

II. Design of the Coupling Coils With an Intermediate Coil

Fig. 1 depicts the proposed coil structure, where the intermediate coil is split into two coils, i.e., L_{T1} and L_{T2}, and it is placed in overlap with the receiver coil L_S on the receiver side to form a compact structure, as shown in Fig. 1(b). It should be noted that all coils are double D coils [11] but with different directions, i.e., L_S and L_{T2} are perpendicular to L_{T1} and L_P, respectively. As a result, the net magnetic flux generated by L_{T1} and L_P passing through L_S and L_{T2} will be zero if the structure is completely symmetrical [12], and vice versa. Therefore, the mutual inductances between those perpendicular coils are almost zero. Inside the perpendicular coils, there are only two mutual inductances, i.e., M_1 between L_{T1} and L_P, and M_2 between L_{T2} and L_S. To simplify the design, L_{T1} is designed to be equal to L_{T2}, i.e., $L_{T1} = L_{T2} = L_T$.

III. Circuit Topology

The circuit diagram of the proposed WPT system is illustrated in Fig. 2, where a reconfigurable intermediate resonant circuit is formed by two additional switches S_1 and S_2 that can be

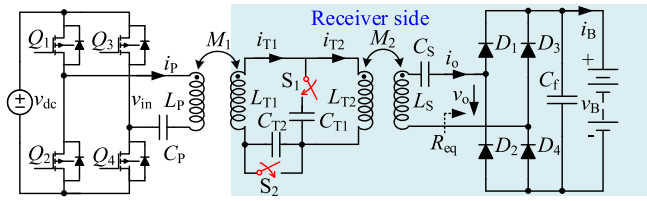

Fig. 2. Circuit diagram of the proposed WPT system based on a reconfigurable intermediate resonant circuit.

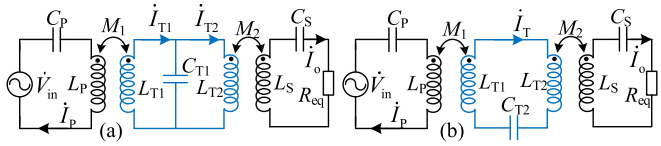

Fig. 3. Equivalent circuits of the proposed WPT system. (a) When S_1 and S_2 are turned ON. (b) When S_1 and S_2 are turned OFF.

the low-cost and compact relays [13]. As shown in Fig. 3, two intermediate resonant circuits can be obtained, resulting in two operating modes of the proposed WPT system. C_P, C_{T1}, C_{T2}, and C_S are the resonant capacitors, which should satisfy the following equation to tune the WPT system:

$$\begin{cases} C_P = (\omega^2 L_P)^{-1} & C_{T2} = \left[\omega^2 (L_{T1} + L_{T2})\right]^{-1} \\ & \quad = \left[2\omega^2 L_T\right]^{-1} \\ C_S = (\omega^2 L_S)^{-1} & C_{T1} = (\omega^2 L_{T1})^{-1} = (\omega^2 L_{T2})^{-1} \\ & \quad = (\omega^2 L_T)^{-1} \end{cases} \tag{1}$$

where ω is the operating frequency of the proposed WPT system.

The relationship between the input and output of the inverter and the rectifier can be expressed as [10]

$$\begin{cases} V_{\text{in}} = 2\sqrt{2}V_{\text{dc}}/\pi & V_o = 2\sqrt{2}V_B/\pi \\ I_o = \pi\sqrt{2}I_B/4. \end{cases} \tag{2}$$

A. Circuit Modeling and Analysis in CC Mode

Fig. 3(a) shows the equivalent circuit of the proposed WPT system when S_1 and S_2 are turned ON, where R_{eq} is the equivalent resistance of the rectifier, i.e., $R_{\text{eq}} = 8R_L(\pi^2)^{-1}$ [10]. According to Kirchhoff's voltage Law (KVL) and the mutual coupling theory, the system can be expressed as

$$\begin{cases} \dot{V}_{\text{in}} = [-jX_{\text{CP}} + jX_{\text{LP}}]\,\dot{I}_P + jX_{M1}\dot{I}_{T1} \\ 0 = -jX_{M1}\dot{I}_P + jX_{\text{LT}}\dot{I}_{T1} - jX_{\text{CT1}}(\dot{I}_{T1} - \dot{I}_{T2}) \\ 0 = jX_{\text{CT1}}(\dot{I}_{T1} - \dot{I}_{T2}) - jX_{\text{LT}}\dot{I}_{T2} + jX_{M2}\dot{I}_o \\ 0 = -jX_{M2}\dot{I}_{T2} + (jX_{\text{LS}} - jX_{\text{CS}} + R_{\text{eq}})\,\dot{I}_o \end{cases} \tag{3}$$

where

$$\begin{cases} X_{\text{LP}} = \omega L_P & X_{\text{CP}} = 1/\omega C_P \quad X_{\text{LT}} = \omega L_T \\ X_{\text{CT1}} = 1/\omega C_{T1} & \\ X_{M1} = \omega M_1 & X_{M2} = \omega M_2 \quad X_{\text{LS}} = \omega L_S \\ X_{\text{CS}} = 1/\omega C_S. & \end{cases} \tag{4}$$

Substituting (1) and (4) into (3), the following equations can be obtained:

$$\begin{cases} \dot{I}_o = \dot{V}_{\rm in} L_T / j\omega M_1 M_2 \\ \dot{V}_o = \dot{I}_o R_{\rm eq} = \dot{V}_{\rm in} L_T R_{\rm eq} / j\omega M_1 M_2 \\ \dot{I}_P = \dot{V}_{\rm in} R_{\rm eq} {L_T}^2 / \omega^2 {M_1}^2 {M_2}^2 \\ Z_{\rm in} = \dot{V}_{\rm in} / \dot{I}_1 = \omega^2 {M_1}^2 {M_2}^2 / R_{\rm eq} {L_T}^2. \end{cases} \tag{5}$$

Then, substituting (2) into (5), the dc output current can be obtained as

$$I_B = 8 V_{\rm dc} L_T / \pi^2 \omega M_1 M_2. \tag{6}$$

It is clear from (6) that the output current of the proposed WPT system I_B is irrelevant to the load $R_{\rm eq}$. Instead, it is determined by the inherent parameters, i.e., L_T, M_1, M_2, the input dc voltage $V_{\rm dc}$, and the operating frequency ω. Once these parameters are designed and fixed, the output current can be considered as a constant current source, which is suitable for charging battery in the CC stage. Meanwhile, the input impedance seen from the inverter is purely resistive, which indicates that this WPT structure can achieve ZPA with fixed operating frequency by using the resonant compensations. Therefore, the inverter only provides active power to the load, which can lower the power rating, i.e., current stress or voltage stress of the power devices [10].

B. Circuit Modeling and Analysis in CV Mode

The circuit structure becomes the one shown in Fig. 3(b) by turning OFF S_1 and S_2. Similarly, by using KVL and the mutual coupling theory, the following equations can be obtained:

$$\begin{cases} \dot{V}_{\rm in} = \left[-jX_{\rm CP} + jX_{\rm LP}\right] \dot{I}_P + jX_{M1} \dot{I}_T \\ 0 = -jX_{M1} \dot{I}_P + \left(jX_{\rm LT} - jX_{\rm CT2} + jX_{\rm LT}\right) \dot{I}_T + jX_{M2} \dot{I}_o \\ 0 = -jX_{M2} \dot{I}_T + \left(jX_{\rm LS} - jX_{\rm CS} + R_{\rm eq}\right) \dot{I}_o. \end{cases} \tag{7}$$

Substituting (1) and (4) into (7), the currents and voltages can be described as

$$\begin{cases} \dot{I}_o = \dot{V}_{\rm in} M_2 / R_{\rm eq} M_1 \qquad \dot{V}_o = \dot{I}_o R_{\rm eq} = \dot{V}_{\rm in} M_2 / M_1 \\ \dot{I}_P = \dot{V}_{\rm in} {M_2}^2 / R_{\rm eq} {M_1}^2 \quad Z_{\rm in} = \dot{V}_{\rm in} / \dot{I}_P = {M_1}^2 / R_{\rm eq} {M_2}^2. \end{cases} \tag{8}$$

Similarly, substituting (2) into (8), the dc output voltage can be calculated as

$$V_B = V_{\rm dc} M_2 / M_1. \tag{9}$$

Interestingly, the dc output voltage V_B is independent of the load $R_{\rm eq}$in this case. It can be considered as a constant voltage source, provided that $V_{\rm dc}$, M_1, and M_2 are fixed. It can be used to charge battery in the CV stage. The inverter can also achieve ZPA with fixed operating frequency.

C. Control and Discussion

The control diagram for the proposed WPT system is provided in Fig. 4, where k and V_B are the voltage gain and reference charging voltage in the CV mode, respectively. Low-cost relay

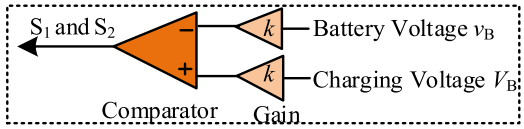

Fig. 4. Control diagram for S_1 and S_2.

can be used as the switches S_1 and S_2. When the battery voltage v_B is smaller than the reference charging voltage V_B, i.e., $v_B < V_B$, the driving signals of S_1 and S_2 are high level to turn ON S_1 and S_2 so that the system operates in the CC mode. Then, when the battery voltage reaches the reference charging voltage during the charging process, the driving signals of S_1 and S_2 become low level. The charging mode will be changed to CV mode by turning OFF S_1 and S_2.

As we can find from the above analysis, the proposed WPT system can work either in CC mode or CV mode by flexibly reconfiguring the intermediate resonant circuit with the help of the additional switches, and, both two operation modes can achieve ZPA, which can lower the power rating of the power devices by only providing active power to the load. Thanks to the additional switches installed on the receiver side, the communication between the transmitter side and the receiver side is not needed in the proposed WPT system. This not only can save the cost but also can improve the stability.

It can be found from (6) and (9) that both I_B and V_B are highly related to the mutual inductances M_1 and M_2. Therefore, the variations of M_1 or M_2 caused by misalignments will affect the accuracy of the charging current I_B and the charging voltage V_B. This is the limitation of the proposed idea. Therefore, this proposed method is suitable for those applications where the receiving coil can be easily aligned with the transmitting coil, e.g., electronic bicycles (EBs) [10], [13] and hence, M_1 and M_2 can be easily fixed and nearly constant.

It should be noted that the CC and CV characteristics can also be derived by using the gyrator-based analysis method [14].

IV. Parameters Design

In the first step, the charging current I_B and charging voltage V_B should be chosen according to the requirement of the battery. Then, the dc input voltage $V_{\rm dc}$ should be chosen. Finally, according to (6) and (9), the mutual inductances can be calculated as

$$\begin{cases} M_1 = \sqrt{8 {V_{\rm dc}}^2 L_T / \pi^2 \omega V_B I_B} \\ M_2 = \sqrt{8 V_B L_T / \pi^2 \omega I_B}. \end{cases} \tag{10}$$

The finite-element analysis software Maxwell plays an important role in designing the coupling coils [10], [11], [13]. The size of the coil will be first determined by the available installation space of various applications. Then, L_T can be determined, and the turns of the intermediate coil can be calculated by Maxwell to achieve the desired L_T. Finally, required mutual inductances can be achieved by varying the turns of the transmitter coil and the receiver coil using Maxwell [10], [11], [13]. The flow chart of designing the coils is shown in Fig. 5.

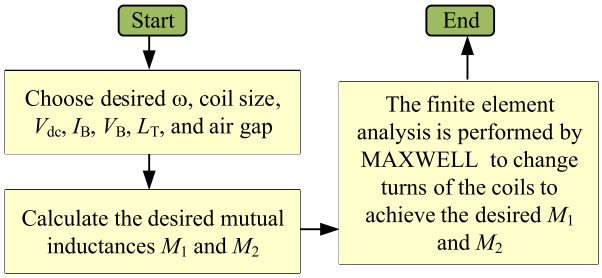

Fig. 5. Flow chart of designing the coils.

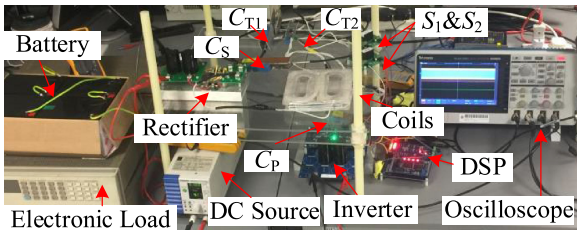

Fig. 6. Experimental setup.

TABLE I
SYSTEM SPECIFICATION AND PARAMETER VALUES

V_{dc}	L_P	L_{T1}	L_{T2}	L_S	M_1
60V	22.17μH	18.02μH	18.02μH	6.94μH	9.82μH
M_2	C_P	C_{T1}	C_{T2}	C_S	f
7.87μH	4.57nF	5.62nF	2.81nF	14.60nF	500kHz

In this letter, the input dc voltage is chosen as 60 V (V_{dc} = 60 A). The operating frequency is 500 kHz. L_T is chosen as 18 μH in this letter as an example. Four batteries manufactured by the RS Pro are connected in a series as the load [15]. The recommended maximum charging current and charging voltage for the load are 3.6 A ($I_B = 3.6$ A) and 48 V ($V_B = 48$ A), respectively [15]. The dimensions of the coupling coils are shown in detail in Fig. 1, where the airgap is selected as 20 mm which is suitable for applications such as EBs [10]. To reduce the cost, ferrite cores are not used in this letter. Then, the turns of L_P, L_{T1}, L_{T2}, and L_S are calculated as 11, 8, 8, 4 to achieve the desired mutual inductances by using Maxwell.

V. EXPERIMENTAL VERIFICATIONS

The experimental prototype is depicted in Fig. 6. The detailed parameters are given in Table I. Fig. 7(a) shows the key experimental waveforms in CC mode, where the dc output current is kept at ∼3.6 A. The inverter can achieve both ZPA and ZVS in CC mode, as shown in Fig. 7(a) and (b), which agrees well with the theoretical analysis.

The CC mode will be changed into CV mode when the battery voltage is increased to 48 V. It can be found from Fig. 8 that the CC mode can be smoothly changed to the CV mode by using the relay switches. The corresponding experimental waveforms when the system operates in the CV mode are shown in Fig. 9. From Fig. 9, the charging voltage can be maintained at ∼48 V,

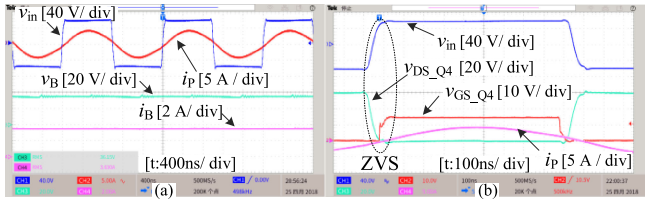

Fig. 7. Experimental waveforms in CC mode. (a) Waveforms of v_{in}, i_P, v_B, and i_B. (b) Waveforms of Q_4.

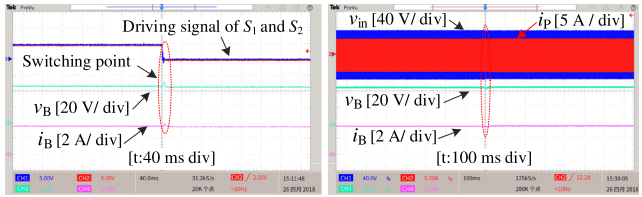

Fig. 8. Transient waveforms from CC mode to CV mode. (a) Waveforms of the driving signals of S_1 and S_2. (b) Waveforms of v_{in}, i_P, v_B, and i_B.

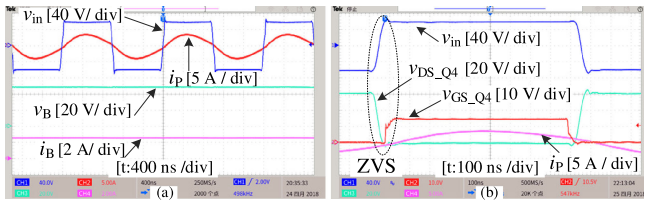

Fig. 9. Experimental waveforms in CV mode. (a) Waveforms of v_{in}, i_P, v_B, and i_B. (b) Waveforms of Q_4.

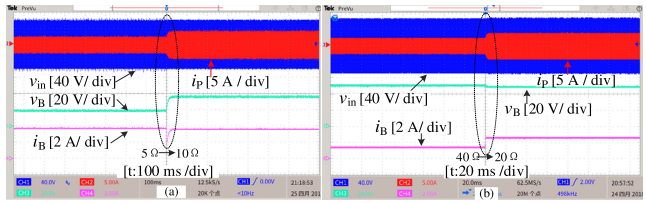

Fig. 10. Dynamic performance of the proposed WPT system. (a) In CC mode when the load changes from 5 to 10 Ω. (b) In CV mode when load changes from 40 to 20 Ω.

and the charging current decreases during the CV charging process. Once again, the WPT system can achieve ZPA and ZVS in the CV mode.

In order to test the robust performance of the proposed WPT system when the load is suddenly changed, the battery is replaced by the electronic load as the load. It can be found in Fig. 10(a) and (b) that the proposed WPT system can maintain a constant output current in the CC mode and a constant output voltage in the CV mode when the load changes.

The measured experimental results in terms of charging current, charging voltage, and the overall efficiency during the entire charging profile are shown in Fig. 11(a) and (b), respectively. The maximum charging efficiency is 92.25%, which is acceptable for battery charging applications. The charging current will decrease during the CV charging process. In other words, the equivalent resistance of battery significantly

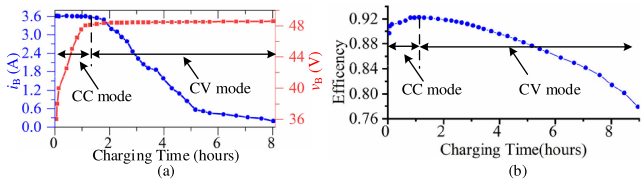

Fig. 11. Experimental results. (a) Measured charging profile. (b) Measured efficiencies.

increases during the CV charging process. Therefore, it leads to the WPT system works in light-load conditions, i.e., the output power drops in CV mode, which results in a low efficiency during the CV mode. Finally, the charging process will be completed with the charging current decreases to nearly zero.

VI. Conclusion

A reconfigurable intermediate resonant circuit based WPT is presented to charge batteries. The intermediate coil is split into two coils to form a reconfigurable intermediate resonant circuit. The intermediate coil is placed in overlap with the receiver coil, which makes the coupling coil structure much simpler and more compact than the previous approaches. Both CC and CV modes can realize ZPA and ZVS, simultaneously. An experimental prototype is built to verify the effectiveness of the proposed method, and the experimental results verify the validity of the theoretical analysis.

References

[1] S. Ping, A. P. Hu, S. Malpas, and D. Budgettt, "A frequency control method for regulating wireless power to implantable devices," *IEEE Trans. Biomed. Circuits Syst.*, vol. 2, no. 1, pp. 22–29, Mar. 2008.

[2] K. W. Klontz, D. M. Divan, D. W. Novotny, and R. D. Lorenz, "Contactless power delivery system for mining applications," *IEEE Trans. Ind. Appl.*, vol. 31, no. 1, pp. 27–35, Jan./Feb. 1995.

[3] J. Kuipers, H. Bruning, S. Bakker, and H. Rijnaarts, "Near field resonant inductive coupling to power electronic devices dispersed in water," *Sens. Actuators A, Phys.*, vol. 178, pp. 217–222, May 2012.

[4] Y. Li, R. Mai, L. Lu, and Z. He, "Active and reactive currents decomposition based control of angle and magnitude of current for a parallel multiinverter IPT system," *IEEE Trans. Power Electron.*, vol. 32, no. 2, pp. 1602–1614, Feb. 2017.

[5] A. Khaligh and Z. Li, "Battery, ultracapacitor, fuel cell, and hybrid energy storage systems for electric, hybrid electric, fuel cell, and plug-in hybrid electric vehicles: State of the art," *IEEE Trans. Veh. Technol.*, vol. 59, no. 6, pp. 2806–2814, Jul. 2010.

[6] Y. Nagatsuka, N. Ehara, Y. Kaneko, S. Abe, and T. Yasuda, "Compact contactless power transfer system for electric vehicles," in *Proc. Int. Power Electron. Conf.*, Sapporo, Japan, 2010, pp. 807–813.

[7] C.-S. Wang, G. A. Covic, and O. H. Stielau, "Power transfer capability and bifurcation phenomena of loosely coupled inductive power transfer systems," *IEEE Trans. Ind. Electron.*, vol. 51, no. 1, pp. 148–157, Feb. 2004.

[8] W. Zhang, S. C. Wong, C. K. Tse, and Q. Chen, "Analysis and comparison of secondary series- and parallel-compensated inductive power transfer systems operating for optimal efficiency and load-independent voltage-transfer ratio," *IEEE Trans. Power Electron.*, vol. 29, no. 6, pp. 2979–2990, Jun. 2014.

[9] X. Qu, H. Han, S. C. Wong, C. K. Tse, and W. Chen, "Hybrid IPT topologies with constant current or constant voltage output for battery charging applications," *IEEE Trans. Power Electron.*, vol. 30, no. 11, pp. 6329–6337, Nov. 2015.

[10] R. Mai, Y. Chen, Y. Li, Y. Zhang, G. Cao, and Z. He, "Inductive power transfer for massive electric bicycles charging based on hybrid topology switching with a single inverter," *IEEE Trans. Power Electron.*, vol. 32, no. 8, pp. 5897–5906, Aug. 2017.

[11] Y. Li, T. Lin, R. Mai, L. Huang, and Z. He, "Compact double-sided decoupled coils based WPT systems for high power applications: analysis, design and experimental verification," *IEEE Trans. Transp. Electrific.*, vol. 4, no. 1, pp. 64–75, Mar. 2018.

[12] I. Ghotbi, M. Najjarzadegan, H. Sarfaraz, S. J. Ashtiani, and O. Shoaei, "Enhanced power-delivered-to-load through planar multiple-harmonic wireless power transmission," *IEEE Trans. Circuits Syst. II, Express Briefs*, 2018, early access.

[13] Y. Li, J. Hu, F. Chen, S. Liu, Z. Yan, and Z. He, "A new-variable-coil-structure-based IPT system with load-independent constant output current or voltage for charging electric bicycles," *IEEE Trans. Power Electron.*, vol. 33, no. 10, pp. 8226–8230, Oct. 2018.

[14] Y. H. Sohn, B. H. Choi, G.-H. Cho, and C. T. Rim, "Gyrator-based analysis of resonant circuits in inductive power transfer systems," *IEEE Trans. Power Electron.*, vol. 31, no. 10, pp. 6824–6843, Oct. 2016.

[15] RS Pro 537–7305+Datasheet. 2018. [Online]. Available: https://docs-apac.rs-online.com/webdocs/1580/0900766b81580e6f.pdf